IMPROVING THE THEORETICAL FOUNDATIONS OF THE MULTI-MODE TRANSPORT MODEL

Glenn Bateman, Arnold H. Kritz, Aaron J. Redd, Matteo Erba
Gregory Rewoldt,[1] Jan Weiland,[2] P¨arStrand,[2] Jon E. Kinsey,[3] and Bruce Scott[4]
Lehigh Universit yPhysics Department
16 Memorial Drive East, Bethlehem, PA 18015

Abstract

A new version of the Multi-Mode transport model, designated MMM98, is being developed with improved theoretical foundations, in an ongoing effort to predict the temperature and density profiles in tokamaks. For transport near the edge of the plasma, MMM98 uses a new model based on 3-D nonlinear simulations of drift Alfvén mode turbulence. Flow shear stabilization effects have been added to the Weiland model for Ion Temperature Gradient and Trapped Electron Modes, which usually dominates in most of the plasma core. For transport near the magnetic axis at high beta, a new kinetic ballooning mode model has been constructed based on FULL stability code computations.

The Multi-Mode transport model is a combination of theory-based transport models used to predict the temperature and density profiles in tokamaks [1]–[7]. The previous version of the Multi-Mode model, designated MMM95 [1], predicted experimentally measured profiles with a relative rms deviation of less than 15% in L-mode and H-mode discharges from TFTR, DIII-D, and JET [3, 4]. The objective of the present research is to improve the theoretical foundations of the Multi-Mode model by using a new combination of theoretically derived models.

A new model has been developed for transport near the edge of the plasma based on 3-D nonlinear turbulence simulations [8]. This edge turbulence consists of $\mathbf{E} \times \mathbf{B}$ convective cells driven by "drift Alfvén" modes. The transport fluxes (Q_i^{DA} = ion thermal flux, Q_e^{DA} = electron thermal flux, and , $_i^{DA}$ = ion particle flux) computed by these turbulence simulations are fitted as follows:

$$\begin{aligned} Q_i^{DA} &= -1.57\, n_e T_e c_s (\rho_s/R)^2 (T_i/T_e)^{2.233} \\ &\quad \times (1.25 - 0.25\hat{\beta}/20)(\hat{\beta}/20) \\ &\quad \times [0.12 g_{ph}^2 + 1.64 g_{ph} g_{nh} + 0.24 g_{nh}^2] \\ &\quad \times \exp[-3.1236(\kappa - 1.6)]/(0.6 + 0.4\hat{s}^2) \end{aligned}$$

$$\begin{aligned} Q_e^{DA} &= -0.458\, n_e T_e c_s (\rho_s/R)^2 \exp[1.1224(T_i/T_e - 1)] \\ &\quad \times (1.25 - 0.25\hat{\beta}/20)(\hat{\beta}/20) \\ &\quad \times [0.3 g_{pe}^2 + 0.8 g_{pe} g_{ne} + 1.2 g_{ne}^2] \\ &\quad \times \exp[-3.1236(\kappa - 1.6)]/(0.6 + 0.4\hat{s}^2) \end{aligned}$$

$$\begin{aligned} , \,{}_i^{DA} &= -0.189\, n_e c_s (\rho_s/R)^2 g_p^2 \exp[1.0015(T_i/T_e - 1)] \\ &\quad \times (1.25 - 0.25\hat{\beta}/20)(\hat{\beta}/20) \\ &\quad \times [0.032 g_{pe}^2 - 0.13 g_{pe} g_{ne} + 4.13 g_{ne}^2] \\ &\quad \times \exp[-3.1236(\kappa - 1.6)]/(0.6 + 0.4\hat{s}^2) \end{aligned}$$

[1]Plasma Physics Laboratory, Princeton Universit y, Princeton, NJ 08543-0451
[2]Chalmers University of Tec hnology, Göteborg, Sweden
[3]Oak Ridge Associated Universities, Oak Ridge, TN.
Present address: General Atomics, P. O. Box 85608, San Diego, CA 92186-5608
[4]Max-Planck Institut f¨ ur Plasmaphysik, Euratom Association, D-85748 Garching, Germany

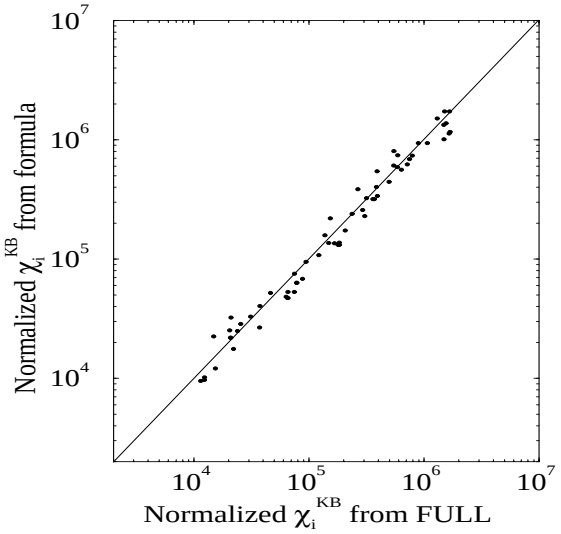

Fig. 1. Dots show the effective ion thermal diffusivity given by the fitting formula Eq. 1 compared with FULL code compuations. The line is a guide representing a perfect fit.

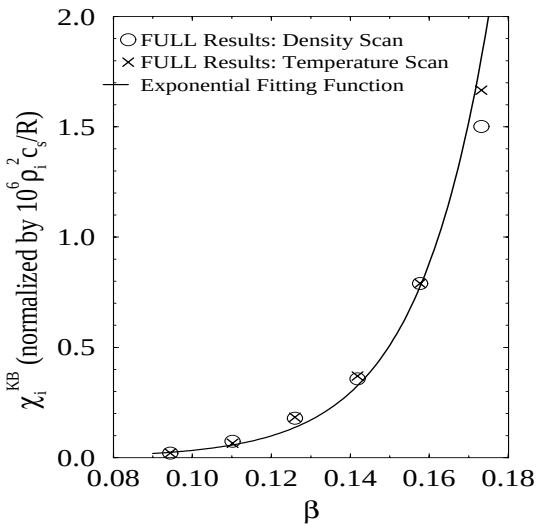

Fig. 2. Ion thermal diffusivity as a function of local beta given by the fitting formula Eq. 1 (solid line) and by FULL code computations (open circles and crosses).

where $c_s = \sqrt{T_e/M_i}$, $\rho_s = \sqrt{T_e M_i}/(eB)$, R = major radius, $g_p = -R(dp/dr)/p$, $p = n_e T_e + n_i T_i$, (correspondingly $p_h = n_h T_h$ is the hydrogenic thermal pressure with hydrogenic density n_h and temperature T_h with normalized gradient $g_{ph} = -R(dp_h/dr)/p_h$, and $p_e = n_e T_e$ is the electron pressure), $\hat{\beta} = \beta_e q^2 g_{pe}^2$, $\beta_e \equiv n_e T_e 2\mu_0/B^2$, q = safety factor, κ = local elongation, and $\hat{s} \approx r(dq/dr)/q$ is the magnetic shear. From these expressions, it can be seen that the transport produced by this model decreases rapidly with plasma elongation. The strong scaling with pressure gradient to the fourth power and magnetic q^2 results in more transport near the plasma edge than in the core. This model has gyro-Bohm scaling.

Flow shear stabilization has been implemented in the Weiland model for transport driven by drift waves which usually dominates in the core of the plasma [1]. These drift waves include Ion Temperature Gradient and Trapped Electron Modes. The flow shear rate [9] is subtracted from each of the eigenvalue growth rates computed in the Weiland model. The eigenfunctions are not affected by this change.

A new kinetic ballooning mode transport model has been developed from computations with the FULL code [10, 11] to describe transport near the magnetic axis, where the ITG mode is generally stable. These comprehensive linear stability calculations are fully electromagnetic in nature, and include effects from trapped and untrapped particles, finite banana-orbit width, Landau damping and finite Larmor radius. A transport model was constructed from FULL code stability computations covering the following range of parameters: $0.094 \le \beta \le 0.177$, $0.96 \le \kappa \le 1.70$, $-0.036 \le \delta \equiv$ triangularity ≤ 0.060, $3.7 \le (-R/p)(dp/dr) \le 4.46$, $0.085 \le \epsilon \equiv r/R \le 0.119$, $0.679 \le q \le 1.027$, $0.355 \le \hat{s} \le 0.738$, $0.75 \le T_i/T_e \le 1.5$, $0.0 \le n_s/n_e \le 0.15$, where n_s is the fast ion deuterium density, and $0.0 \le n_c/n_e \le 0.06$, where n_c is the carbon impurity density. This range of parameters is appropriate near the magnetic axis in tokamak discharges.

The resulting fitting function for the new kinetic ballooning mode model effective ion thermal diffusivity χ_i^{KB} is:

$$\begin{aligned} \chi_i^{\mathrm{KB}} \quad \propto \quad & (c_s \rho_i^2/R)[-R(dp/dr)/p]^3 (1-\hat{s})(q-0.61)^2 \mathrm{e}^{(62.8)\beta} \mathrm{e}^{-(30)\delta} \mathrm{e}^{-(100)\epsilon} \\ & \times \max[e^{-9.5(\kappa-1.6)}, 1]\,[0.848 - n_s/n_e] \\ & \times \left[(T_i/T_e - 0.753)^2 + 3.46\right] \left[(0.0516 - n_c/n_e)^2 + 0.0591\right] \end{aligned} \tag{1}$$

The ratio between the electron and ion thermal diffusivities is:

$$\begin{aligned}\chi_e^{\mathrm{KB}}/\chi_i^{\mathrm{KB}} &= (1.43\times10^5)\,(1.45-\kappa)\,(\beta-0.090)\,(\epsilon-0.111)\\ &\quad\times(q-0.576)\,(\delta-0.00775)\,(2.42-n_s/n_e)\\ &\quad\times(17.7+T_i/T_e)\,(0.299-n_c/n_e)\end{aligned}\tag{2}$$

The ratio between the hydrogenic ion particle diffusivity and the ion thermal diffusivity is

$$\begin{aligned}D_h^{\mathrm{KB}}/\chi_i^{\mathrm{KB}} &= 2430\,[0.134-(\kappa-1.1)^2]\,(0.153-\epsilon)\,(q-0.293)\\ &\quad\times((\min[\beta,0.125]-0.088)^2+0.00113)\\ &\quad\times(1.49-n_s/n_e)\,(4.48-T_i/T_e)\,(1.0+n_c/n_e)\end{aligned}\tag{3}$$

Finally, for carbon impurity transport:

$$D_Z^{\mathrm{KB}}/\chi_i^{\mathrm{KB}} = (-0.60)\,(0.25-n_c/n_e)\tag{4}$$

The dependences of the kinetic ballooning transport on the ten study parameters were assumed to be separable. The validity of this assumption was verified with multiple scans in the parameter space. When the diffusivities given by the fitting functions (Eqs. 1–4 above) were compared with the corresponding FULL code calculations, the average relative rms deviation was found to be 22%, with an offset of -3%. This comparison is shown in Fig. 1 for the ion thermal diffusivity.

The beta dependence of the kinetic ballooning mode is shown in Fig. 2. The circles and crosses show results from the FULL code scanning beta by changing density and temperature separately. The strong exponential beta dependence of Eq. 1 is shown by the solid curve. There appears to be no marginal stability point for this mode.

The effect of flow shear stabilization is shown in Fig. 3, which is a simulation of an "optimized shear" JET discharge 40847 before the H-mode phase. The lowest (dotted) curve shows the simulation results using the Multi-Mode model MMM95 and the other two curves (dashed and solid) results from the same model with one times and five times the the flow shear rate subtracted from the Weiland model growth rates. The dots are TRANSP analyzed experimental data.

In this simulation, the flow shear rate is given by

$$\omega_{E\times B} = \frac{(RB_\theta)^2}{B}\left(\frac{\partial}{\partial\psi}\right)\frac{E_r}{RB_\theta} \quad \text{where} \quad E_r = (Z_i e n_i)^{-1}\,\nabla P_i - v_{\theta_i}B_\Phi + v_{\Phi_i}B_\theta$$

The poloidal magnetic field B_θ and total magnetic field B are taken at the major radius R of the geometric center of each flux surface, and ψ is the steam function $\psi_{pol}/2\pi$. The pressure gradient and variables other than the velocity are computed self-consistently in this BALDUR transport simulation. The toroidal velocity is taken from experimental data and the poloidal velocity is neglected.

Fig. 4 shows a simulation using the new MMM98 model described in this paper (solid curves) compared with experimental data (dots and circles with error bars) for an L-mode TFTR discharge 50911 from one of the ρ_* scans. The drift Alfvén and Weiland models are taken with coefficients equal to unity. The kinetic ballooning mode model is calibrated to provide a small amount of transport near the magnetic axis where ITG and other modes are stable.

In conclusion, a new Multi-Mode transport model MMM98 has been developed. Preliminary simulations have been carried out with this model.

Acknowledgments

This work was supported by the U.S. Department of Energy, under Contract No. DE-FG02-92-ER-54141.

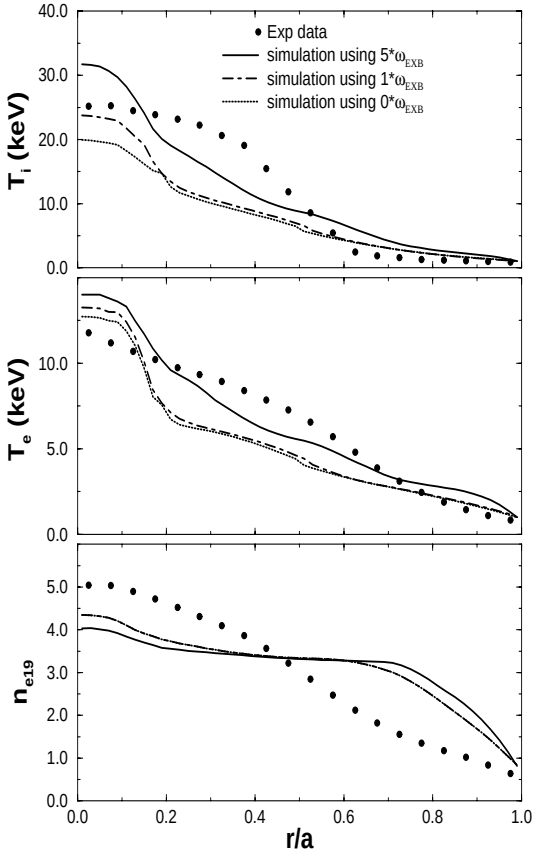

Fig. 3. Ion temperature, electron temperature, and electron density profiles from a BALDUR transport simulation (solid lines) compared against experimental data (dots) as a function of major radius for JET discharge 40847 at 46.5 seconds.

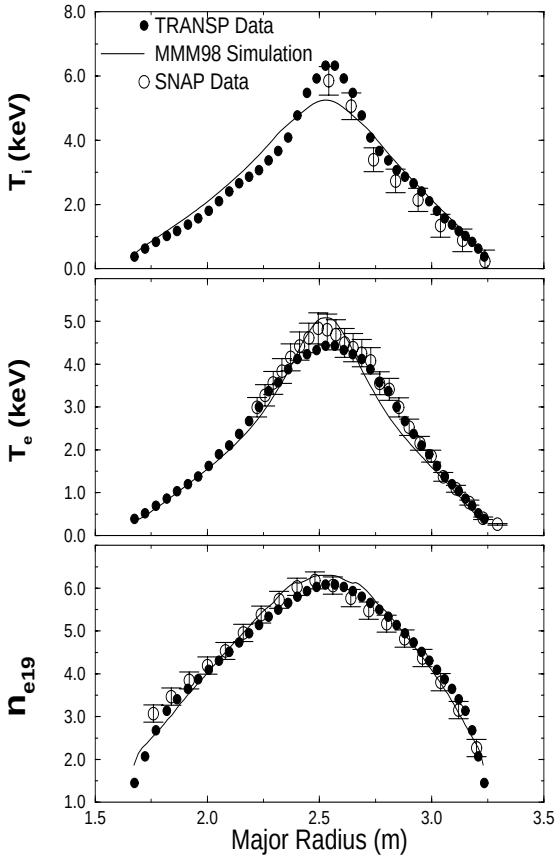

Fig. 4. Ion temperature, electron temperature, and electron density profiles from a BALDUR transport simulation (solid lines) compared against experimental data (dots and circles) as a function of major radius for TFTR discharge 50911 at 3.94 seconds.

References

[1] G. Bateman, A. H. Kritz, J. E. Kinsey, A. J. Redd, and J. Weiland, Phys. Plasmas **5,** 1793 (1998).

[2] A. H. Kritz, G. Bateman, A. J. Redd, M. Erba, B. Scott, P. Strand, J. Weiland, *A New Version of the Multi-Mode Transport Model,* European Physical Society Meeting, Prague, Czech Republic, 1998.

[3] G. Bateman, J. E. Kinsey, A. H. Kritz, A. J. Redd, and J. Weiland, *Theory-based transport modelling of tokamak temperature and density profiles,* in *Proceedings of the Sixteenth IAEA Fusion Energy Conference, (Montréal, Canada, 7–11 October)*, Vienna, 1996, IAEA, Vol. 2, pp. 559.

[4] J. E. Kinsey, R. E. Waltz, and D. P. Schissel, *Transport model testing and comparisons using the ITER and DIII-D profile databases,* in *European Physical Society Meeting, Berchtesgaten, Germany June 1997*, European Physical Socienty, Petit-Lancy.

[5] J. E. Kinsey and G. Bateman, Phys. of Plasmas, **3** 3344 (1996).

[6] G. Bateman, J. Weiland, H. Nordman, J. E. Kinsey, and C. Singer, Physica Scripta **51** 591 (1995).

[7] G. Bateman, Phys. Fluids **B 4** (1992) 634.

[8] B. Scott, Plasma Phys. Control. Fusion **39,** 1635–1668 (1997).

[9] T. S. Hahm, and K. H. Burrell, Phys. Plasmas **2,** 1648 (1995).

[10] A. J. Redd, *Pressure-Driven Transport in the Core of Tokamak Plasmas,* PhD thesis, Lehigh University, Bethlehem PA USA (1998).

[11] G. Rewoldt, M. A. Beer, M. S. Chance, T. S. Hahm, Z. Lin, and W. M Tang, Phys. Plasmas **5,** 1815 (1998).